

## Magnetic-Field Effects on the Size of Vortices below the Surface of NbSe<sub>2</sub> Detected Using Low Energy $\beta$ -NMR

Z. Salman,<sup>1,2</sup> D. Wang,<sup>3</sup> K. H. Chow,<sup>4</sup> M. D. Hossain,<sup>3</sup> S. R. Kretzman,<sup>1</sup> T. A. Keeler,<sup>3</sup> C. D. P. Levy,<sup>1</sup> W. A. MacFarlane,<sup>5</sup> R. I. Miller,<sup>1</sup> G. D. Morris,<sup>1</sup> T. J. Parolin,<sup>5</sup> H. Saadaoui,<sup>3</sup> M. Smadella,<sup>3</sup> and R. F. Kiefl<sup>1,3,6</sup>

<sup>1</sup>TRIUMF, 4004 Wesbrook Mall, Vancouver, BC, Canada, V6T 2A3

<sup>2</sup>Clarendon Laboratory, Department of Physics, Oxford University, Parks Road, Oxford OX1 3PU, United Kingdom

<sup>3</sup>Department of Physics and Astronomy, University of British Columbia, Vancouver, BC, Canada V6T 1Z1

<sup>4</sup>Department of Physics, University of Alberta, Edmonton, AB, Canada T6G 2J1

<sup>5</sup>Chemistry Department, University of British Columbia, Vancouver, BC, Canada V6T 1Z1

<sup>6</sup>Canadian Institute for Advanced Research, Canada

(Received 14 June 2006; published 16 April 2007)

A low energy radioactive beam of polarized <sup>8</sup>Li has been used to observe the vortex lattice near the surface of superconducting NbSe<sub>2</sub>. The inhomogeneous magnetic-field distribution associated with the vortex lattice was measured using depth-resolved  $\beta$ -detected NMR. Below  $T_c$ , one observes the characteristic line shape for a triangular vortex lattice which depends on the magnetic penetration depth and vortex core radius. The size of the vortex core varies strongly with the magnetic field. In particular, in a low field of 10.8 mT, the core radius is much larger than the coherence length. The possible origin of these giant vortices is discussed.

DOI: 10.1103/PhysRevLett.98.167001

PACS numbers: 74.25.Qt, 74.25.Ha, 76.60.-k, 76.75.+i

The vortex state of a superconductor exhibits many fascinating properties. A fundamental feature, which follows from the topology of the superconducting ground state and electron pairing, is that each vortex carries an elementary quantum of magnetic flux  $\phi_0 = hc/2e$ . In the simple Ginzburg-Landau model, the order parameter for superconductivity is zero at the vortex core and rises to the bulk value on the scale of the coherence length, while the magnetic field falls away from the core on the scale of the London penetration depth. However, even in conventional superconductors, vortices are complex objects with properties that were not anticipated when they were first predicted by Abrikosov [1]. For example, Caroli *et al.* proposed the existence of bound quasiparticles associated with an isolated vortex [2] which were eventually observed with STM measurement on NbSe<sub>2</sub> [3]. Thermal deoccupation of these bound states leads to shrinking of the vortex core at low temperatures or Kramer-Pesch (KP) effect [4]. Muon spin rotation ( $\mu$ SR) has been used extensively to measure the magnetic-field distribution in the vortex state which is a sensitive probe of the vortex properties. For example,  $\mu$ SR results on NbSe<sub>2</sub> [5] have shown that the low temperature core radius is significantly larger than predicted in the quantum limit [6]. Recently, there has been considerable work on the role of delocalized quasiparticles and the interaction between vortices, particularly in multiband superconductors such as NbSe<sub>2</sub> and MgB<sub>2</sub>, where there is more than one superconducting gap. It is believed such effects are responsible for the unusually large and field dependent specific heat [7] and thermal conductivity [8] in the vortex state.

In this Letter, we report observation of giant vortices near the surface of superconducting NbSe<sub>2</sub> using a novel

method of low energy  $\beta$ -detected NMR ( $\beta$ -NMR) [9,10]. Below  $T_c$ , we observe a broad asymmetric  $\beta$ -NMR line shape, which is characteristic of a triangular lattice of magnetic vortices. As in the case of  $\mu$ SR, the internal field distribution, as reflected by the line shape, is sensitive to the magnetic penetration depth and vortex core radius. Surprisingly, the fitted core radius of 77(10) nm is much larger than the coherence length ( $\sim$ 10 nm) in a small magnetic field of 10.8 mT. We propose the extended nature of the vortices originates from multiband effects and thermal vibrations of the vortices.

The low energy (30 keV) beam of <sup>8</sup>Li is produced at the isotope separator and accelerator (ISAC) at TRIUMF. A large nuclear polarization (70%) is generated inflight using a collinear optical pumping method. The  $\beta$ -NMR spectrometer sits on a high voltage platform so that the implantation energy can be varied between 1–30 keV, corresponding to an average implantation depth between 5–150 nm. In  $\beta$ -NMR, the nuclear polarization is monitored through the anisotropic  $\beta$  decay. In the case of <sup>8</sup>Li, which has a mean lifetime of 1.2 s, the emitted betas have an average energy of about 6 MeV, so that they easily pass through stainless steel windows in the ultrahigh vacuum (UHV) chamber. The magnetic resonance is detected by monitoring the time-averaged nuclear polarization as a function of a small perpendicular radio frequency magnetic-field. <sup>8</sup>Li is a spin  $I = 2$  nucleus with a small electric quadrupole moment  $Q = +33$  mB and gyromagnetic ratio  $\gamma = 6.302$  MHz/T. In the absence of a quadrupolar splitting, the line shape is determined by the distribution of local magnetic fields at the Li site.

A single crystal of 2H-NbSe<sub>2</sub>, measuring about 4 mm in diameter and 0.1 mm thick, was attached to a sapphire plate

and mounted on a cold finger cryostat. It had a sharp superconducting transition at  $T_c = 7.0$  K with a width of 0.1 K. The sample was cleaved just prior to introduction into the UHV ( $10^{-9}$  torr); such short exposure to air has no effect on our  $\beta$ -NMR measurements. The beam was focused onto the sample so that there was no detectable background signal from the sapphire.

Figure 1(a) shows the  $\beta$ -NMR spectrum in the normal state of NbSe<sub>2</sub> in a magnetic field of 300 mT applied along the  $c$  axis and beam direction, which are both perpendicular to the surface. Above  $T_c = 7.0$  K, the line shape is nearly independent of magnetic field  $H$ , temperature, and mean implantation depth  $\langle z \rangle$ . In a previous study, we showed that in the normal state, there is no resolved quadrupolar splitting and the Korringa relaxation is anomalously small compared to simple metals such as Ag [11]. The observed line width is attributed to nuclear dipolar broadening from the <sup>93</sup>Nb nuclear moments. These results suggest that Li occupies a site in the van der Waals gap between the NbSe<sub>2</sub> layers and is only weakly coupled to the conduction band.

After field-cooling below  $T_c$ , the resonance broadens asymmetrically (see Fig. 1(b)) and exhibits the features characteristic of a triangular vortex lattice in a superconductor. In particular, note the most probable frequency, or cusp frequency, shifts by an amount  $\Delta_c$  below the normal state frequency. The cusp frequency (or magnetic field) arises from Li located midway between two adjacent vortices. In addition, there is a high frequency tail which corresponds to the magnetic-field distribution near the vortex core. The high frequency cutoff, which is shifted by an amount  $\Delta_v$  above the normal state frequency, corre-

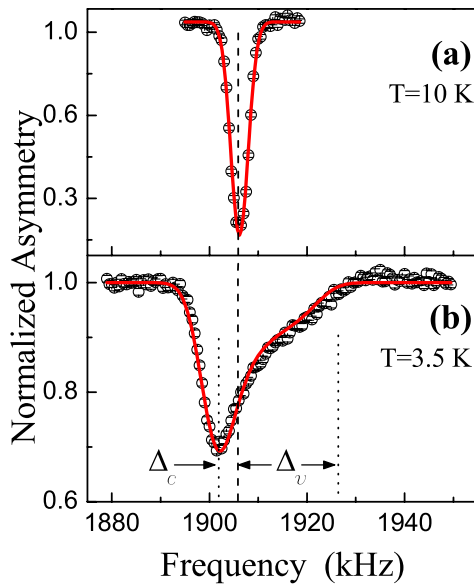


FIG. 1 (color online).  $\beta$ -NMR spectra in a magnetic field of 300 mT and with beam energy of 20 keV, corresponding to a mean implantation depth  $\langle z \rangle = 85$  nm. (a) In the normal state at 10 K and (b) field cooled to 3.5 K or  $0.5T_c$ .

sponds to the field at the vortex core. At high implantation energies, we expect the magnetic field distribution (frequency distribution) to be close to that in a bulk superconductor. Such bulk field distributions have been studied extensively with  $\mu$ SR and used to extract the magnetic penetration depth and vortex core radius. In applied magnetic fields ( $H \ll H_{c2}$ ), the local magnetic field at position  $\mathbf{r} = (x, y)$  relative to a vortex can be decomposed into its Fourier components:

$$B(\mathbf{r}) = B_0 \sum_{\mathbf{k}} C(k, \rho) \frac{e^{-i\mathbf{k}\cdot\mathbf{r}}}{1 + \lambda_{ab}^2 k^2}, \quad (1)$$

where the sum is over all reciprocal lattice vectors of the vortex lattice,  $\lambda_{ab}$  is the in-plane penetration depth,  $\rho$  is the vortex core radius,  $B_0$  is the average magnetic field, and  $C(k, \rho)$  is a phenomenological cutoff function which characterizes the shape and size of the vortex core [12].  $\rho$  is a function of the coherence length  $\xi_{ab}$ , but may also depend on the electronic structure of the vortex and vortex-vortex interactions. The best fit [13] of the current data is with a simple Gaussian cutoff  $C(k, \rho) = \exp[-\frac{1}{2}k^2\rho^2]$  which gives  $\lambda_{ab} = 230(30)$  nm and  $\rho = 13(1)$  nm. These parameters depend slightly on the model for  $C(k, \rho)$ . For example, using a Bessel function cutoff [14] gives  $\lambda_{ab} = 230(30)$  nm and  $\rho = 11(1)$  nm. Previous  $\mu$ SR work on bulk NbSe<sub>2</sub> [15] obtained  $\lambda_{ab} \approx 170$  and  $\rho \approx 12$  at the same field and temperature, using a Bessel function cutoff. The agreement is reasonable considering there are substantial differences in the experimental methods, the form of the raw data and resulting analysis. For example,  $\beta$ -NMR spectra are acquired in the frequency domain rather than in the time domain for  $\mu$ SR. Thus, important features such as  $\Delta_v$  and  $\Delta_c$  are evident in the raw  $\beta$ -NMR data without processing or analysis. Also, in  $\beta$ -NMR, there is no detectable background that interferes with the signal. On the other hand, the form of the field distribution is more complicated as explained below.

Figure 2 shows  $\beta$ -NMR spectra measured in a lower magnetic field of 10.8 mT. The normal state resonance (Fig. 2(a)) is very similar to that observed at 300 mT. The spectra in the superconducting state (Figs. 2(b) and 2(c)) show a strong dependence on temperature (not shown) and  $\langle z \rangle$ . Several important features are evident from Figs. 2(b) and 2(c) without any fitting. First,  $\Delta_c$  decreases as  $\langle z \rangle$  changes from 85 nm (Fig. 2(c)) to 8 nm (Fig. 2(b)). Such narrowing of the field distribution near the surface is understandable since the vortex lattice must approach that of a bulk superconductor deep inside the material, whereas any line broadening from the vortex lattice must vanish well outside the material. The actual crossover begins when the mean depth becomes comparable to  $a_0/2\pi$  where  $a_0[\text{nm}] = 1546/\sqrt{B_{\text{ext}}[\text{mT}]}$  is the mean spacing between vortices[16]. Second,  $\Delta_c$  in Fig. 2(c) has increased by about 50% compared to the corresponding line shape at 300 mT shown in Fig. 1(b).

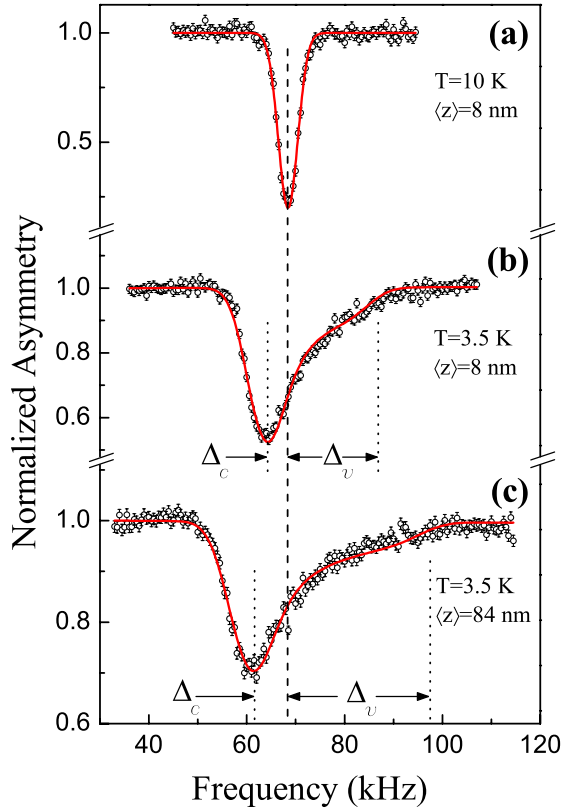


FIG. 2 (color online).  $\beta$ -NMR spectra in a low magnetic field of 10.8 mT. (a) In the normal state at 10 K with a beam energy which corresponds to  $\langle z \rangle = 8$  nm. (b) The same conditions as (a) except field cooled to  $0.5T_c$ . (c) The same temperature as (b), but  $\langle z \rangle$  is about 10 times larger.

This is also consistent with the vortex lattice model since the vortices are further apart in low field.

The most unexpected feature in the data is the remarkable similarity between the line shapes in Figs. 1(b) and 2(b), given the magnetic fields differ by a factor of 27. In particular, in Fig. 2(b), note the cutoff at a frequency  $\Delta_v$  above the normal state frequency. Recall, this corresponds to the frequency (magnetic field) at the vortex core. For example, using  $\rho = 13$  nm and  $\lambda_{ab} = 230$  nm, one finds  $\Delta_v = 76$  kHz or about 3 times larger than what is observed. Typically,  $\Delta_v$  can only be observed in much higher magnetic fields such as in Fig. 1(b) where the vortices are close together. The small value of  $\Delta_v$  in Figs. 2(b) and 2(c) indicates a very extended vortex core where  $\rho \gg \xi_{ab}$ . The possible origin of the oversized vortices is discussed below.

All the data in the superconducting state were fit to a vortex line shape model, which includes effects from the surface. Following Ref. [16], we assume Laplace's equation is valid outside the superconductor, and that a modified London model for a triangular lattice of vortices applies inside the superconductor. This yields a magnetic field at a depth  $z$  equal to

$$B(\mathbf{r}, z) = B_0 \sum_{\mathbf{k}} \frac{C(k, \rho)}{\lambda_{ab}^2 \Lambda^2} \left[ 1 - \frac{k}{\Lambda + k} e^{-\Lambda z} \right] e^{-i\mathbf{k} \cdot \mathbf{r}} \quad (2)$$

where  $\Lambda^2 = k^2 + 1/\lambda_{ab}^2$ . In analogy with bulk superconductors, we include a simple Gaussian cutoff function  $C(k, \rho) = \exp[-\frac{1}{2}k^2\rho^2]$ . For each energy, we calculate a depth-averaged field distribution,

$$\langle n(B) \rangle = \int f(z) n(B, z) dz, \quad (3)$$

where  $f(z)$  is the stopping distribution obtained using the TRIM.SP code to simulate the implantation of  $^8\text{Li}$  in  $\text{NbSe}_2$  [17], and  $n(B, z)$  is the field distribution at a well defined depth  $z$ . The final step is to convolute the resulting frequency spectrum with a Gaussian broadening function which takes into account the nuclear dipolar fields and any residual disorder in the vortex lattice [14]. Typical fits to the model field distribution are shown in Fig. 2. The average frequency equals the normal state frequency implying there is no measurable flux expulsion, which is reasonable for our sample geometry. The measured values for  $\Delta_c$  and  $\Delta_v$  are shown in Fig. 3. For comparison, the solid lines are the best fit to the vortex line shape model assuming a depth independent  $\lambda_{ab}$  and  $\rho$ . At 10.8 mT, we obtain  $\lambda_{ab} = 167(15)$  nm and  $\rho = 77(10)$  nm compared to  $\lambda_{ab} = 230(30)$  nm and  $\rho = 13(1)$  nm at 300 mT. At both fields,  $\Delta_c$  and  $\Delta_v$  behave roughly according to this simple model, but there are clear deviations. In particular,  $\Delta_c$  increases with decreasing  $\langle z \rangle$  close to the surface,

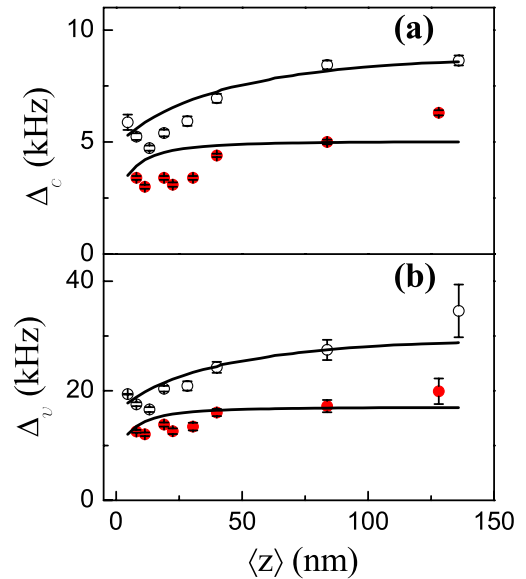


FIG. 3 (color online). Depth dependence of (a) the cusp frequency  $\Delta_c$  and (b) vortex core frequency  $\Delta_v$  relative to the normal state frequency. The open circles are measured in a magnetic field of 10.8 mT, while the filled circles are taken at 300 mT. In all cases, the temperature is 3.5 K which corresponds to  $0.5T_c$ . The solid curves are from the vortex line shape model with a single depth independent  $\lambda_{ab}$  and  $\rho$ .

whereas the simple model predicts a monotonic decrease. Also, both  $\Delta_c$  and  $\Delta_v$  show a stronger variation with depth than the simple model predicts. These are indications that the vortex interactions depend slightly on depth.

The fitted value for  $\lambda_{ab}$  at 10.8 mT is about 30% smaller than at 300 mT and is very close to the  $\mu$ SR results for bulk NbSe<sub>2</sub>. However, the most significant effect of the magnetic field is the extremely large value of  $\rho$  at 10.8 mT. At 300 mT,  $\rho = 13(1)$  nm, which is close to the expected  $\xi_{ab}$  and measurements of  $\rho$  made with  $\mu$ SR in higher fields [15]. At 10.8 mT, the effective  $\rho$  increases to 77(10) nm. It should be stressed that changing the functional form of the line shape produces only small changes in  $\rho$  and has no influence on the ratio between  $\rho$  in high and low field. The magnitude of the effect is much larger than the calculated field dependence of  $\rho$  originating from the bound states which cause the KP effect [18]. It is interesting to compare these results with  $\mu$ SR in bulk NbSe<sub>2</sub>. Early studies in this temperature range showed a substantial increase in  $\rho$  as the field was lowered but the signal was not followed below 100 mT [15]. The field dependence we observe indicates a stronger variation with field below 100 mT than predicted from Ref. [15] where the extrapolated low field value of  $\rho$  was 25 nm at  $0.5T_c$ . Also, very recent work at much lower temperatures (20 mK) gives an extrapolated low field value of 10 nm [19]. A 60% increase in  $\rho$  below 400 mT is attributed to a multiband effect, whereby a second smaller superconducting gap determines the value of  $\rho$  in low fields. In a simple model, with minimal band coupling, the low field  $\xi_{ab} \approx v_F/\pi\Delta_0$  where  $v_F$  is the Fermi velocity and  $\Delta_0$  is the smaller gap. We observe a much larger field dependence to  $\rho$ . The current measurement was made in a lower magnetic field and of course much closer to the surface, but the key difference is likely the temperature. Both angle-resolved photoemission spectroscopy (ARPES) [20] and STM [21] find evidence for a broad distribution of gaps with parts of the Fermi surface showing no measurable gap at higher temperatures near  $T_c$ . The ratio between the maximum and minimum gaps is about five at  $0.5T_c$  [21]. Thermal vibrations of the vortex lattice may also contribute to the observed field dependence in  $\rho$ , since in low magnetic fields the vortices are further apart and less confined by their neighbors. The upturn in  $\Delta_c$  for small  $\langle z \rangle$  (see Fig. 3) indicates some depth dependence to vortex interactions as one approaches the surface. This is consistent with vibrations since the vortex lattice is expected to stiffen very close to the surface, either due to pinning or increased vortex repulsion [22]. A comprehensive theory of the vortices and their interactions, which includes both electronic and vibrational excitations, is needed to resolve the precise origin of this effect.

In conclusion, low energy  $\beta$ -NMR has been used to measure the field distribution of a vortex lattice below the surface of a superconductor. Below  $T_c$  in NbSe<sub>2</sub>, the resonance line is inhomogeneously broadened and has a line shape which is characteristic of a triangular vortex lattice. In a magnetic field of 300 mT, the magnetic penetration depth and core radius are similar to  $\mu$ SR measurements in bulk NbSe<sub>2</sub>. However, in a lower field of 10.8 mT, the vortices are much larger. The multiband nature of the superconductivity and thermal vibrations of the vortices are a possible explanation.

We would like to thank Joe Brill for providing the sample. This research was supported by the Center for Materials and Molecular Research at TRIUMF, NSERC of Canada and the CIAR. We would especially like to acknowledge Rahim Abasalti, Bassam Hitti, Donald Arseneau, and Suzannah Daviel for expert technical support and Jeff Sonier for his critical reading of the manuscript and helpful discussions.

- 
- [1] A. A. Abrikosov, Sov. Phys. JETP **5**, 1174 (1957).
  - [2] C. Caroli, P. G. De Gennes, and J. Matricon, Phys. Lett. **9**, 307 (1964).
  - [3] H. F. Hess *et al.*, Phys. Rev. Lett. **62**, 214 (1989).
  - [4] L. Kramer and W. Pesch, Z. Phys. **269**, 59 (1974).
  - [5] R. I. Miller *et al.*, Phys. Rev. Lett. **85**, 1540 (2000).
  - [6] N. Hayashi *et al.*, Phys. Rev. Lett. **80**, 2921 (1998).
  - [7] J. E. Sonier *et al.*, Phys. Rev. Lett. **82**, 4914 (1999).
  - [8] E. Boaknin *et al.*, Phys. Rev. Lett. **90**, 117003 (2003).
  - [9] G. D. Morris *et al.*, Phys. Rev. Lett. **93**, 157601 (2004).
  - [10] Z. Salman *et al.*, Phys. Rev. Lett. **96**, 147601 (2006); Z. Salman *et al.*, Phys. Rev. B **70**, 104404 (2004).
  - [11] D. Wang *et al.*, Physica B (Amsterdam) **374–375**, 239 (2006).
  - [12] A. Yaouanc, P. Dalmas de Réotier, and E. H. Brandt, Phys. Rev. B **55**, 11107 (1997).
  - [13] The actual fit was done using Eq. (2) and (3), which takes into account the stopping distribution of Li and their proximity to the surface.
  - [14] J. E. Sonier, J. H. Brewer, and R. F. Kiefl, Rev. Mod. Phys. **72**, 769 (2000).
  - [15] J. E. Sonier *et al.*, Phys. Rev. Lett. **79**, 1742 (1997).
  - [16] Ch. Niedermayer *et al.*, Phys. Rev. Lett. **83**, 3932 (1999).
  - [17] W. Eckstein, *Computer Simulation of Ion-Solid Interactions* (Springer, Berlin, 1991).
  - [18] M. Ichioka, A. Hasegawa, and K. Machida, Phys. Rev. B **59**, 184 (1999).
  - [19] F. D. Callaghan *et al.*, Phys. Rev. Lett. **95**, 197001 (2005).
  - [20] T. Yokoya *et al.*, Science **294**, 2518 (2001).
  - [21] J. G. Rodrigo and S. Viera, Physica C (Amsterdam) **404**, 306 (2004).
  - [22] J. Pearl, Appl. Phys. Lett. **5**, 65 (1964); J. Pearl, J. Appl. Phys. **37**, 4139 (1966).